Supplementary Figures and Tables

Supplementary Figure 1. FACS analysis and sorting. (**a**) Gating schemes for representative FACS analyses of control (*Insulin-rtTA*) and p16-expressing (*Insulin-rtTA/tet-p16*) mice (top two rows), and for human islet cells stained for insulin and p16 or isotype control (bottom two rows). (**b**) FACS analysis of islet cells from control and p16 expressing mice stained for pS6; shown are insulin+ cells, red line shows insulin+p16^{+} cells. (**c**) Sorting of GFP^{+} dissociated islet cells from control *Insulin-rtTA/tet-GFP* mice (GFP only) and *Insulin-rtTA/tet-p16/tet-GFP* mice (co-expressing GFP and p16), after 10 d of induction. Cells in the indicated gate were isolated for RNAseq.

Supplementary Figure 2. Expression of proliferation and senescence-associated genes in p16-expressing beta cells. (**a**) Relative mRNA levels of proliferation genes in p16 expressing beta cells, included in downregulated gene sets. Values are mean ± s.e.m. of level in p16-expressing beta cells (grey, $n = 3$) relative to control GFP-expressing beta cells (white, $n = 2$), as derived from RNAseq. (**b**) Relative mRNA levels of senescence-associated genes from upregulated gene sets, in same samples. *t*-test $P < 0.05$ for genes in panels a,b. (**c**) Relative mRNA levels of p53 transcriptional targets in same samples. (**d**) Relative mRNA levels of genes encoding for Cdk inhibitors in same samples. $p16^{Ink4a}$ is endogenous mouse gene. No transcripts of $p19^{ARF}$ were detected. (**e**) Representative images of islet sections of indicated mice stained for p53 (brown) or (**f**) p21 (green).

Supplementary Figure 3. Expression of markers and regulators of beta cell differentiation in p16-expressing beta cells. (**a**–**c**) Representative images of control and p16-expressing islets co-stained for p16 (red) and Nkx6.1, Pdx1 or Chromogranin (Chga) (green). (**d**) Relative mRNA

levels of markers and regulators of beta cell differentiation in GFP (white) and p16-expressing (grey) beta cells, derived from RNA-seq, as in Fig. S1. (**e**) Relative mRNA levels of genes associated with beta cell functional maturation[30] upregulated in p16-expressing beta cells. (**f**) Relative mRNA levels of Polycomb targes, HNF1 targets and nervous system genes associated with beta cell differentiation, upregulated in p16-expressing beta cells. Student's *t*-test $P < 0.05$ for genes in panels e,f.

Supplementary Figure 4. p16 activation and insulin secretion in *Insulin-rtTA/tet-p16* mice – additional data. (**a**) Insulin levels secreted by islets of control (Insulin-rtTA, white) and p16-expressing (Insulin-rtTA/tet-p16, grey) mice incubated in low glucose (2.8 mM) or in low glucose followed by high glucose (16.7 mM) for 1 h. Insulin levels were normalized to the total protein content of each sample following islet lysis. Values are presented relative to the secretion level of control islets at high-glucose, defined as 1, and are mean ± s.d. of five replicates of islets pooled from three mice in each group. (**b**) Insulin levels secreted by islets of control and p16-expressing mice following induction at 6 weeks of age for 2 weeks. Insulin levels were normalized to the insulin content of each sample following islet lysis. Values are presented relative to the secretion level of control islets at high-glucose, defined as 1, and are mean ± s.d. of five replicates of islets pooled from three mice in each group. (**c**) Insulin levels secreted by islets of p16-expressing and control mice following 2 months of tet treatment. Insulin levels were normalized to the insulin content of each sample following islet lysis. Values are presented relative to the secretion level of control islets at high-glucose, defined as 1, and are mean ± s.d. of five replicates of islets pooled from three mice in each group. (**d**) FACS analysis of human p16 expression in islet cells of untreated 10 d-old *Insulin-rtTA/tet-p16* mice (blue), *Insulin-rtTA/tet-p16* mice treated with tet at 5 weeks of age for 10 d (red), and, and WT mice (black).

Low levels of tetracycline-independent p16 expression is observed in untreated mice. Shown are insulin$^+$ cells. (**e**) FACS analysis of human p16 expression in islet cells of *Insulin-rtTA/tet-p16* mice untreated (blue) or treated with tet for 10 d (red) at 6 weeks of age, and of WT mice (black). Shown are insulin$^+$ cells. (**f**) Representative images of pancreatic sections stained for insulin (brown) from indicated mice, untreated. Images are composites. (**g**) Body weights of control and p16-expressing mice following 10 d of p16 induction.

Supplementary Figure 5. p16 activation and insulin secretion in *Pdx1-tTA/tet-p16* mice – additional data. (**a**) FACS analysis of human p16 expression in islet cells of un-induced (tet maintained) *Pdx1-tTA/tet-p16* mice (blue), induced (tet removed for 2 wk) *Pdx1-tTA/tet-p16* mice (red), and WT mice (black). Shown are insulin$^+$ cells. (**b**) FSC-A plot of insulin$^+$ cells from mice shown in Fig. 2d, pooled. Red line shows p16$^+$ cells only. (**c**) Body weights of indicated mice, following 2 weeks of p16 induction. (**d**) Representative images of pancreatic sections stained for insulin (brown) from indicated mice, following p16 induction for indicated times. Images are composites.

Supplementary Figure 6. Changes in beta cell proliferation and GSIS during mouse aging – additional data. (**a**) FACS analysis of Ki67 expression in insulin$^+$ cells of control FVB (WT) and *p16*$^{-/-}$ mice at indicated ages. Cells were pooled from three mice per group. (**b**) Insulin secretion levels at low glucose (2.8 mM) by pancreatic islets of indicated mice, as shown in Fig. 4a with changed Y axis. (**c**) Fold increase in insulin secretion at high versus low glucose conditions by pancreatic islets of WT mice at indicated ages, p16-expressing *Insulin-rtTA/tet-p16* mice (p16OE) and p16$^{-/-}$ mice. Values were calculated based on data shown in Fig. 2a and Fig. 4a,e. (**d**) Sections of *MIP-CreER* and control WT mice stained for human growth hormone, to

exclude protein expression from sequences contained in the transgene. A section of a human pituitary gland was used as a positive control. Dark nuclei in islets are hematoxylin stained.

Supplementary Figure 7. Increased expression of phospho-S6 and mitochondrial proteins in human islets with age. (**a**) Representative images of islet sections of juvenile and adult human subjects at the indicated ages stained for pS6 (white). (**b**) Representative images of islet sections of juvenile and adult human subjects at indicated ages stained for the indicated mitochondrial proteins (white). Images present three islets from each subject.

Supplementary Figure 8. p16 expression levels, cell size and mitochondrial activity in EndoC-βH2 cells. (**a**) Western blot of endogenous p16 in EndoC-βH2 expressing GFP or Cre. (**b**) Western blot analysis of p16 in Cre-expressing EndoC-βH2 (Cre), and in two samples of human islets (Human 1, 2) from middle-aged subjects. (**c**) mRNA levels of *p16*, *Ki67*, and *Insulin* assessed by qRT-PCR in EndoC-βH2 cells expressing the pLKO vector (Vector only), pLKO-puro vector and Cre (Vector + Cre) or shp16 and Cre (shp16 + Cre). (**d**) FACS analysis of Ki67 expression in the indicated cells. (**e**–**f**) FACS analysis of FSC-A (e) and TMRE staining (f) of cells 3 wk after infection with a control GFP vector or with Cre, and treated with the mTOR inhibitor Torin1 or with vehicle (V). (**g**) FACS analysis of TMRE stained cells 3 weeks after infection with an empty pLKO vector or with Cre, and treated with the PPAR-γ inhibitor GW9662 or with vehicle (V).

Supplementary Table 1. Gene expression changes in p16-expressing beta cells. Genes from key gene sets that are preferentially down- or up-regulated in p16-expressing beta cells.

Nature Medicine: doi:10.1038/nm.4054

Supplementary Table 2. Analyzed human samples. Top table includes human subjects whose islet sections were used for immunostains. Bottom table includes subjects whose live islets were used for the indicated FACS stains and analyses.

Supplementary Table 3. Percentages of SA-β-Gal$^+$ cells detected in live dissociated human islets.

Nature Medicine: doi:10.1038/nm.4054

Supplementary Figure 1

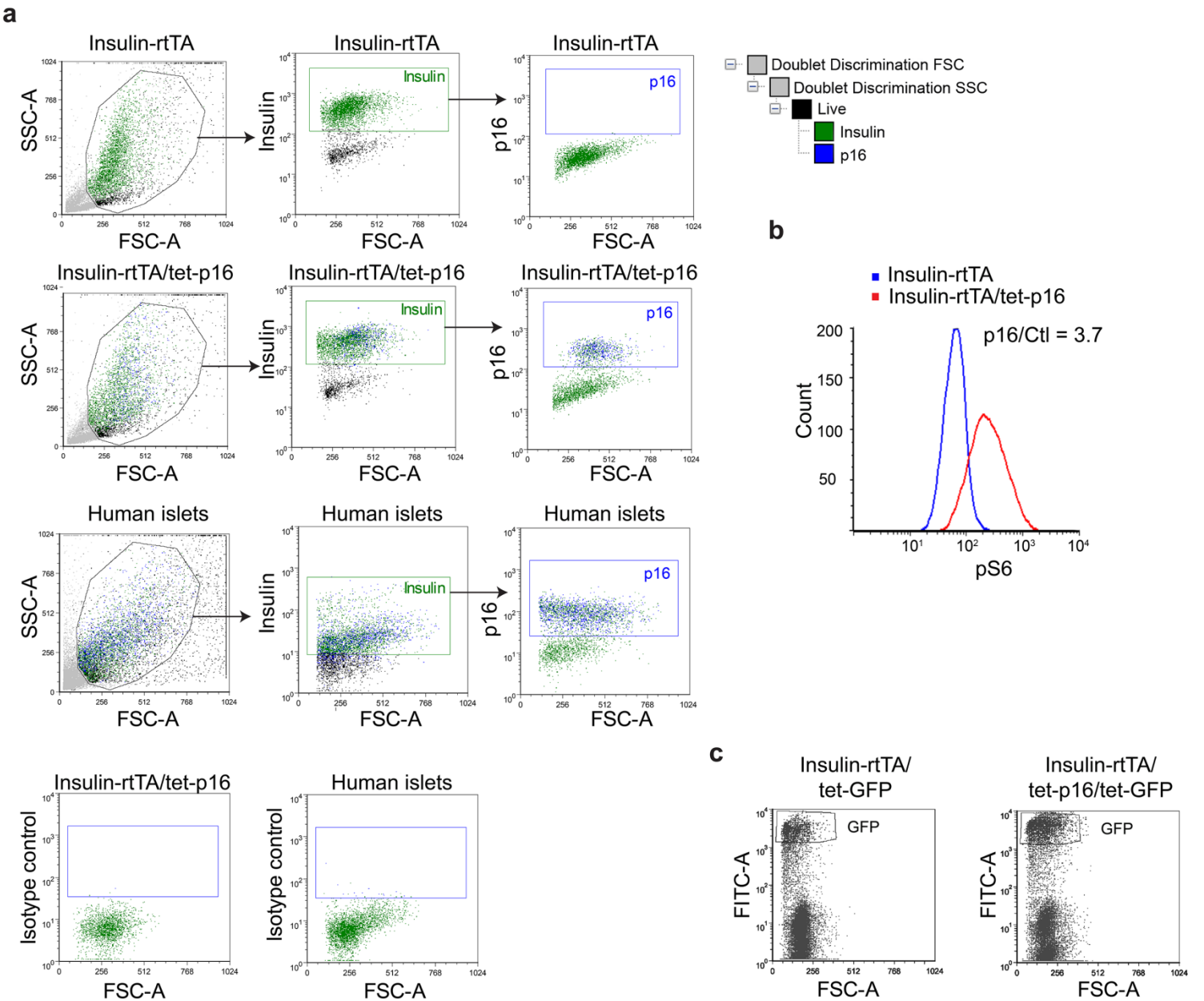

Nature Medicine: doi:10.1038/nm.4054

Supplementary Figure 2

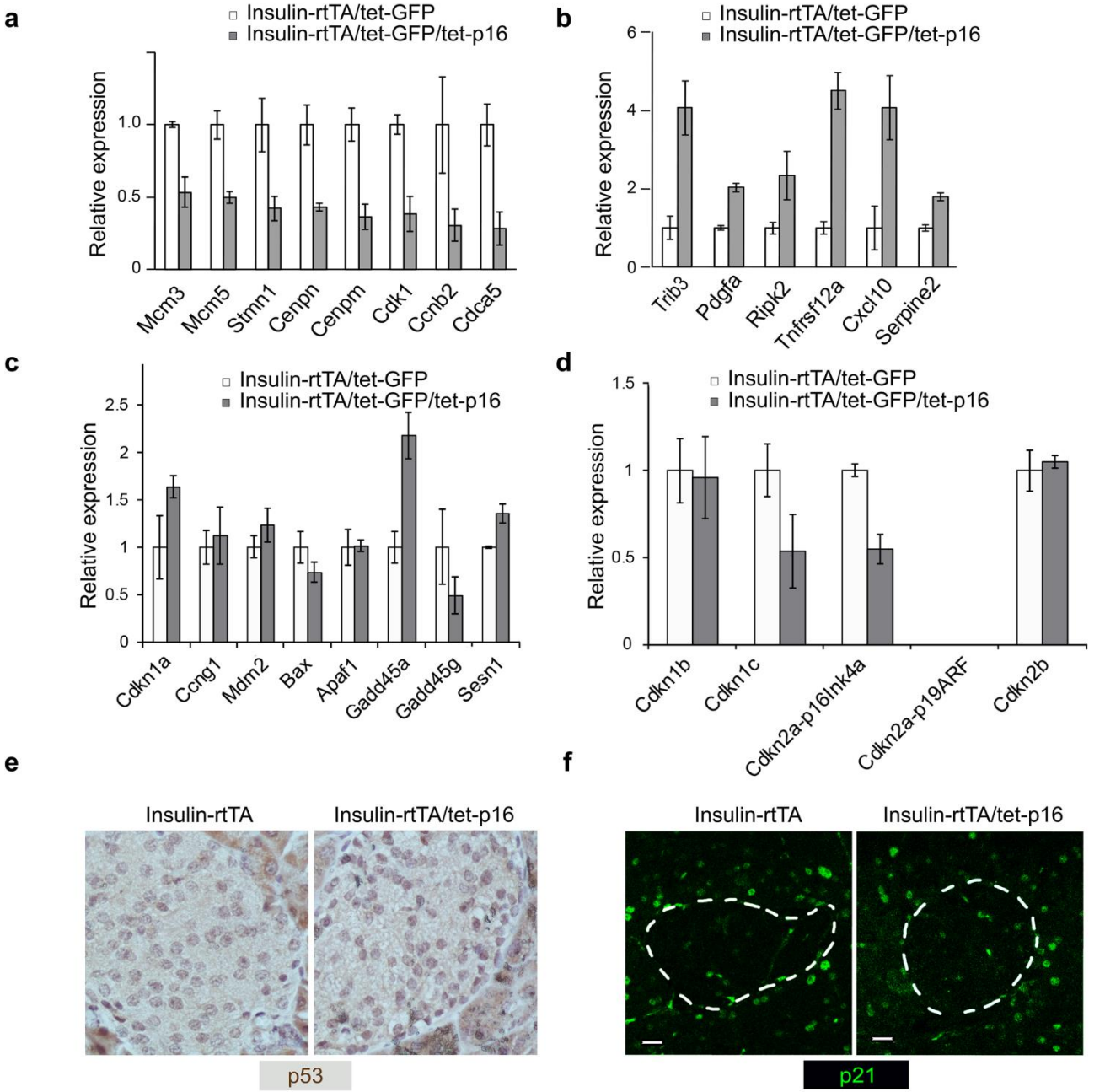

Supplementary Figure 3

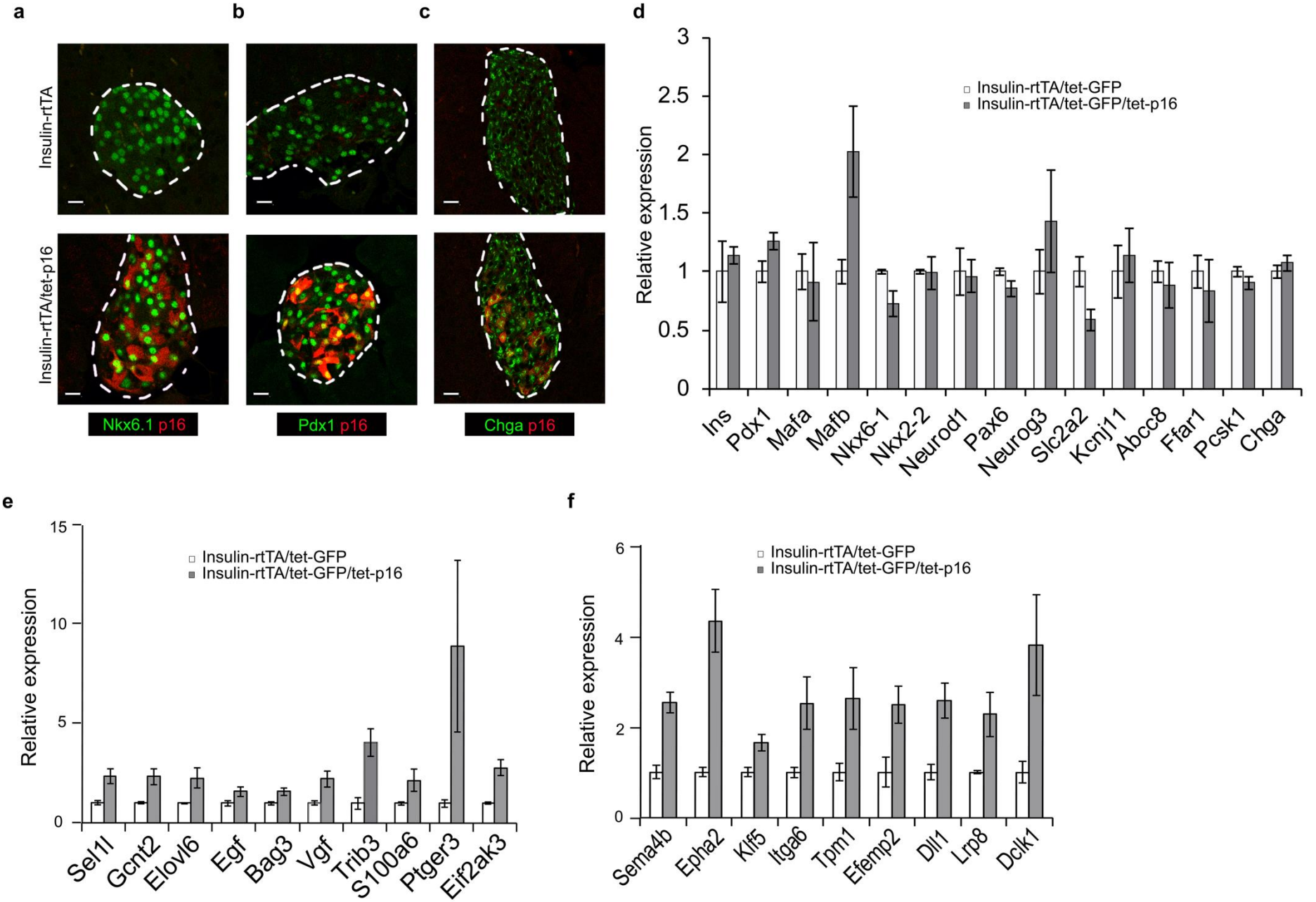

Supplementary Figure 4

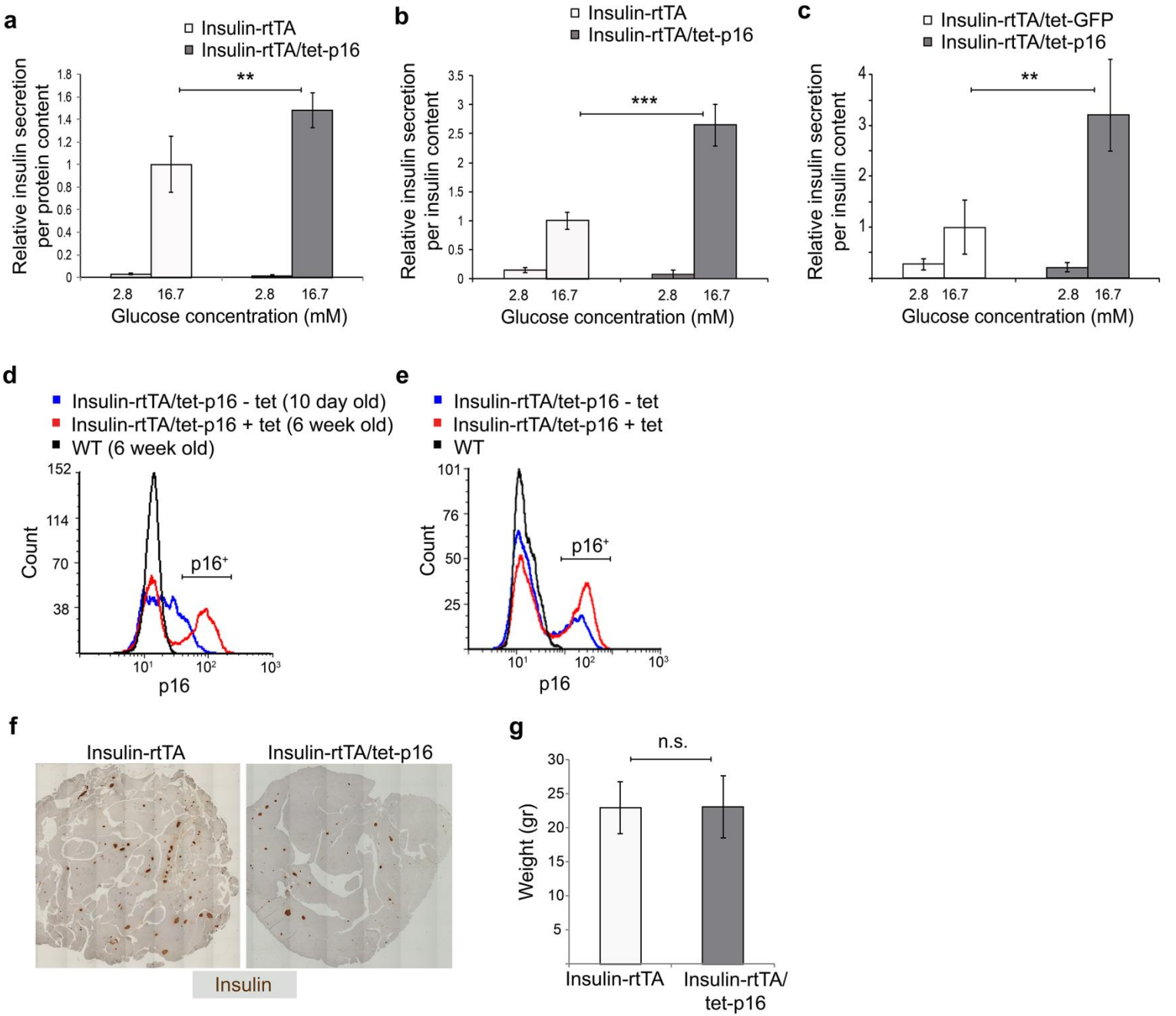

Supplementary Figure 5

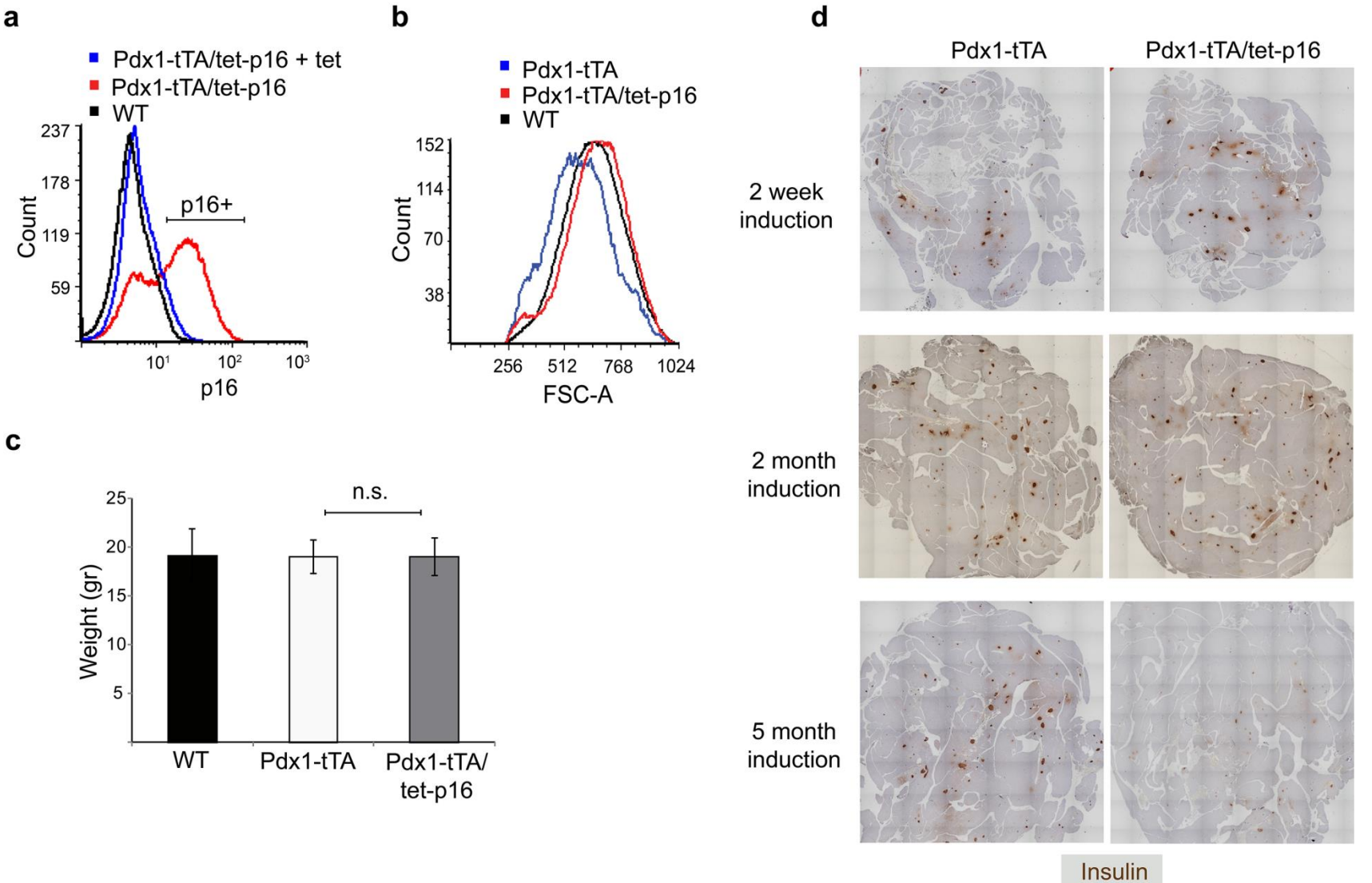

Nature Medicine: doi:10.1038/nm.4054

Supplementary Figure 6

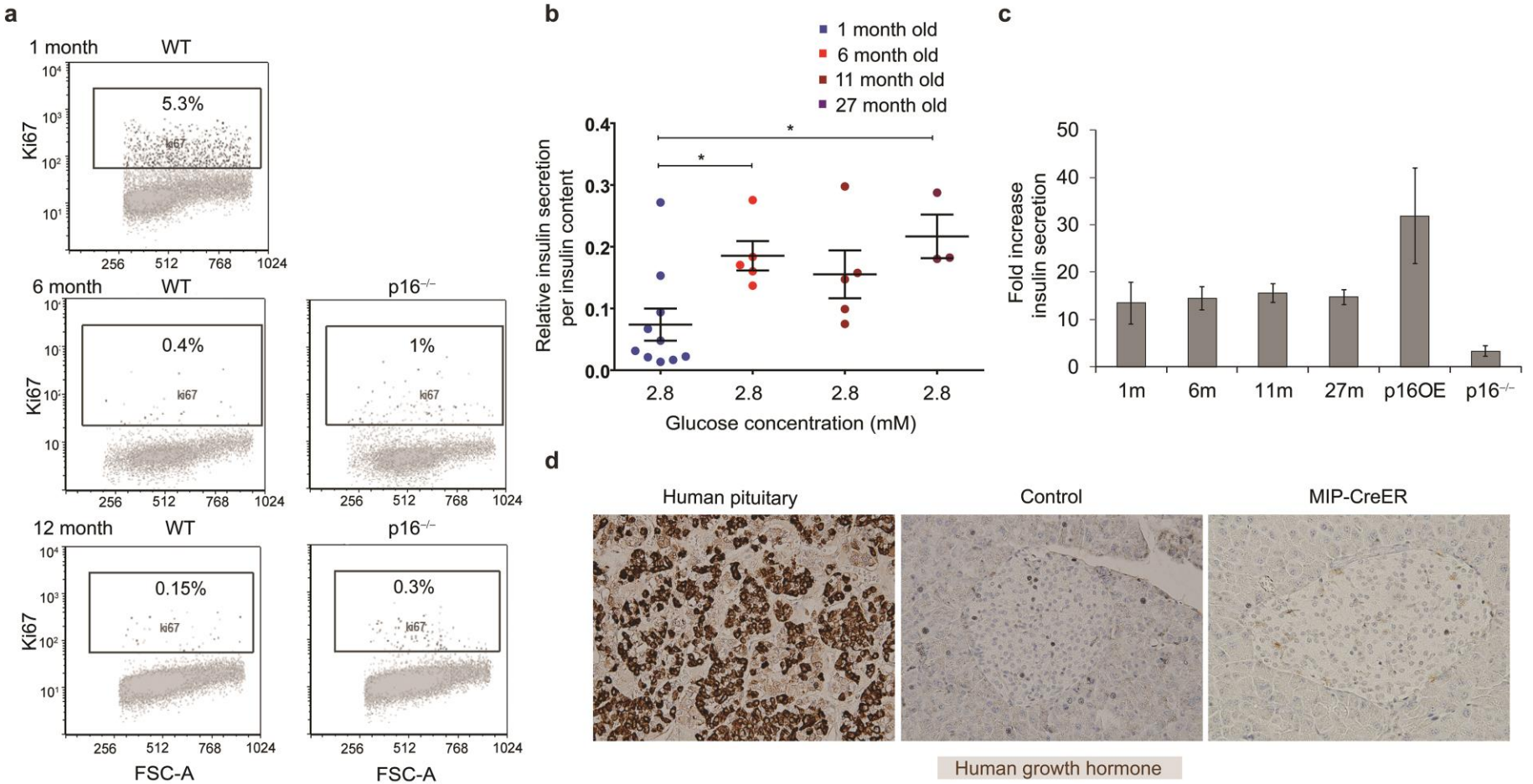

Nature Medicine: doi:10.1038/nm.4054

Supplementary Figure 7

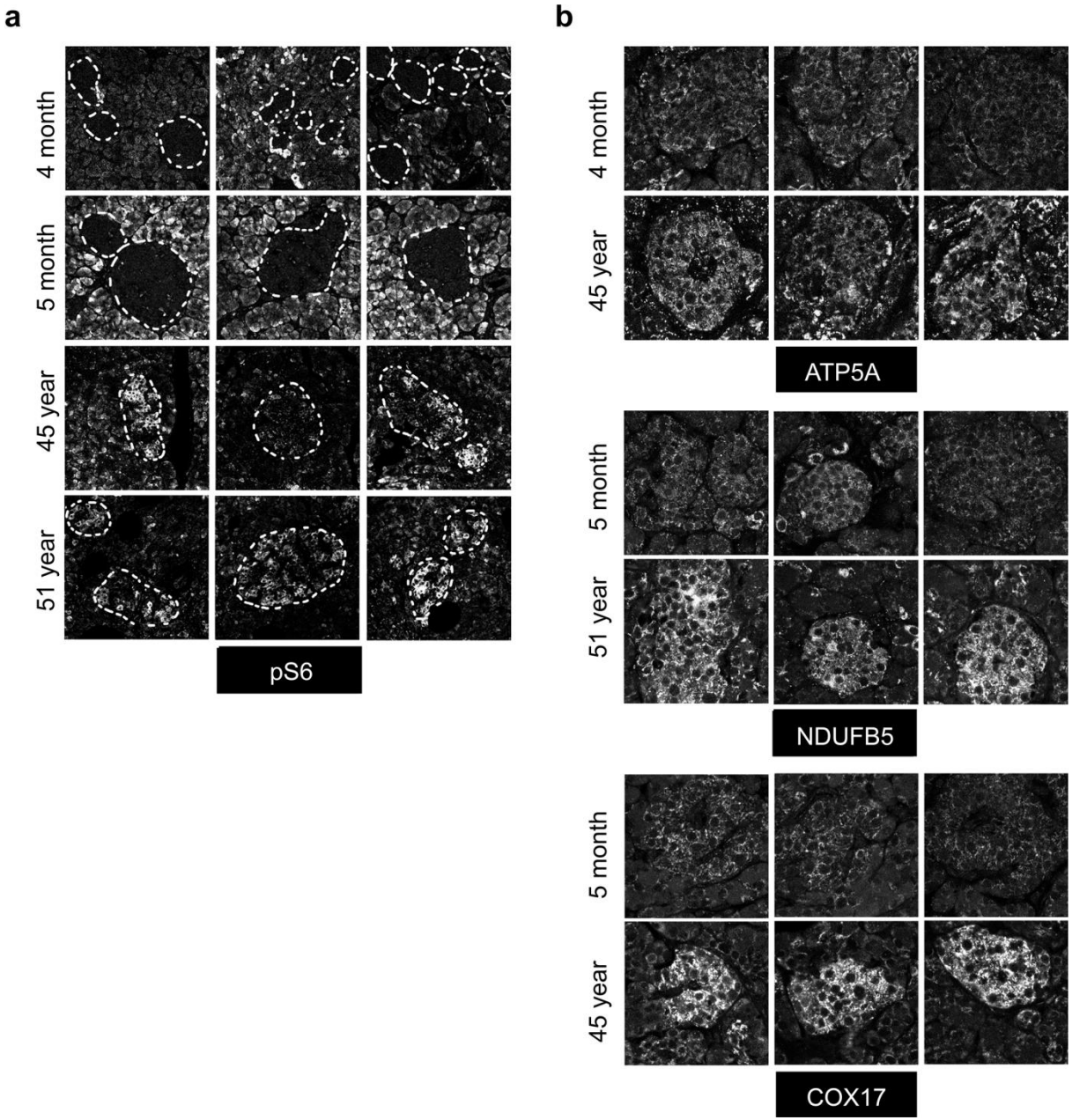

Supplementary Figure 8

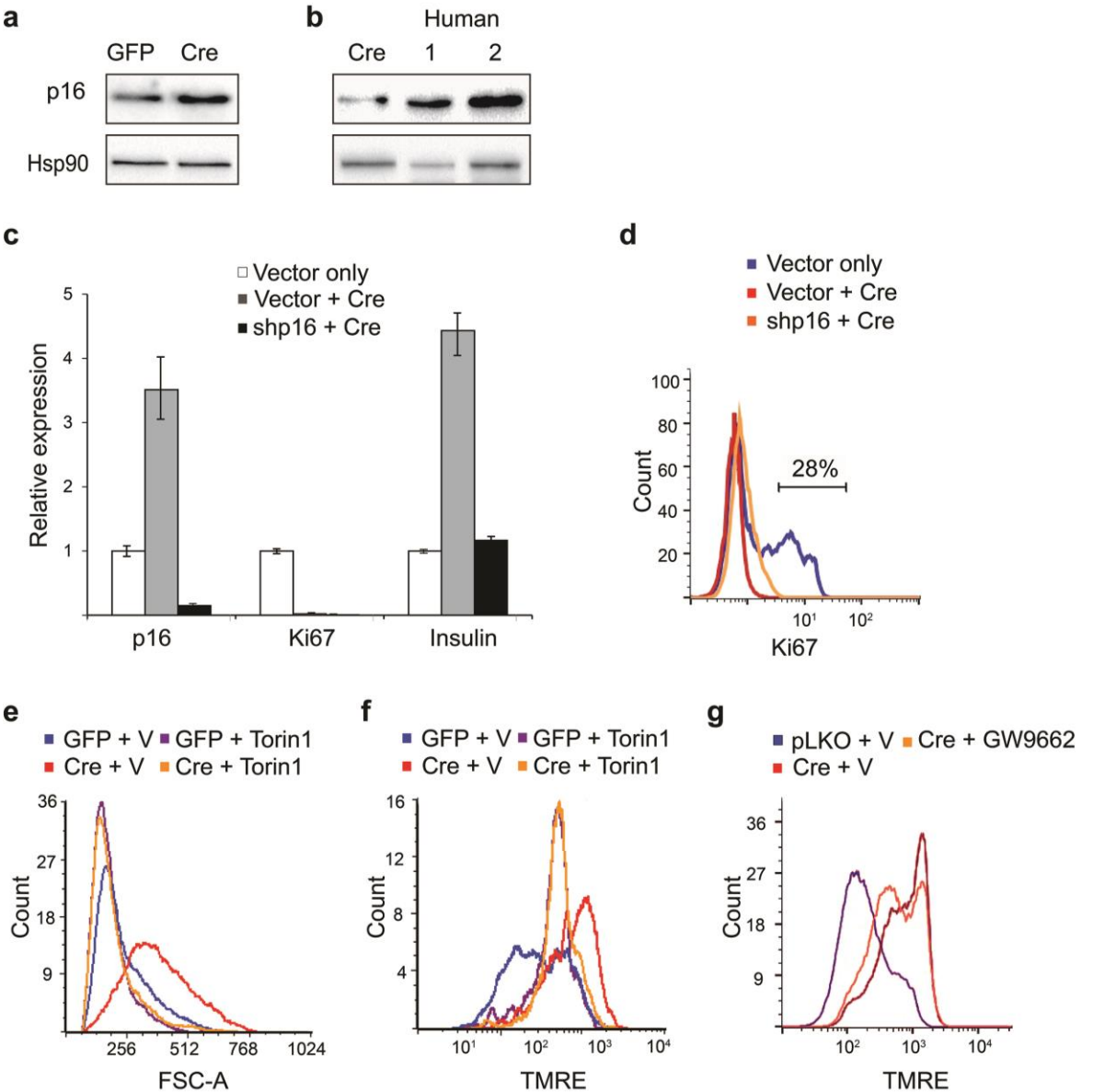

Supplementary Table 2

CaseID	Donor Type	AutoAb (RIA)	Age (years)	Gender	Ethnicity	BMI	Analysis	
6117	No diabetes	Negative	0.33	Male	Caucasian	18.4	Imunnostaining	p16 Cox17 Atp5a pS6
6125	No diabetes	Negative	0.42	Male	Caucasian	18.9	Imunnostaining	p16 Cox17 Ndufb5
6122	No diabetes	Negative	0.42	Female	Caucasian	13.8	Imunnostaining	p16 Cox17 pS6
6107	No diabetes	Negative	2.2	Male	African American	15.9	Imunnostaining	p16 Cox17
6005	No diabetes	Negative	5	Female	Caucasian	15.7	Imunnostaining	p16 Cox17 pS6
6144	No diabetes	Negative	7.5	Female	Hispanic	16.3	Imunnostaining	p16 Cox17
6034	No diabetes	Negative	32	Female	Caucasian	25.2	Imunnostaining	p16 Cox17 pS6
6009	No diabetes	Negative	45	Male	Caucasian	30.6	Imunnostaining	p16 Cox17 Atp5a pS6
6165	No diabetes	Negative	45.8	Female	Caucasian	25	Imunnostaining	p16 Cox17 pS6
6168	No diabetes	No serum available	51	Male	Hispanic	25.2	Imunnostaining	p16 Cox17 Ndufb5 pS6

Case	Donor Age	Donor Gender	Analysis
H1744	56	Female	FACS Insulin p16
H1704	51	Male	FACS C12FDG
H1798	49	Female	FACS p16 and Lamp2a
H1759	48	Male	FACS C12FDG
H1785	42	Male	FACS Insulin and p16
H1851	14	Male	FACS C12FDG
H1852	58	Female	FACS C12FDG and TMRE
H1854	53	Female	FACS C12FDG and TMRE
H1858	57	Male	FACS C12FDG and TMRE

Supplementary Table 3

Case	Donor Age	C12FDG positive cells
H1851	14	2%
H1759	48	54%
H1704	51	60%
H1854	53	52%
H1852	58	44%
H1858	58	40%